

Atmospheric concentration profile reconstructions from radiation measurements

Guillaume Bal and Kui Ren

Department of Applied Physics and Applied Mathematics, Columbia University, New York, NY 10027, USA

E-mail: gb2030@columbia.edu and kr2002@columbia.edu

Received 23 February 2004, in final form 26 October 2004

Published 6 December 2004

Online at stacks.iop.org/IP/21/153

Abstract

We consider the reconstruction of vertical concentration profiles of atmospheric gases from a spectral distribution of radiation measured from a space-borne infrared spectrometer. Under some separability assumptions of the gases' spectral absorption coefficients, we obtain uniqueness results on the reconstruction of concentration profiles from (multiple-wavenumber) radiance measurements and provide an explicit reconstruction procedure. We show that the reconstruction is a *severely ill-posed* problem. To address the reconstruction of localized layers, such as ozone or dust layers, we model the reconstruction of strong localized variations in the concentration profiles by using asymptotic expansions in the layer thickness. Assuming the background is known, we obtain that the location as well as the product of the concentration variability within the layer multiplied and the thickness of the layer may be reconstructed from moderately noisy data. The reconstructions of both the concentration and the thickness of the layer require more accurate data.

1. Introduction

The vertical concentrations of atmospheric gases such as carbon monoxide (CO), carbon dioxide (CO₂) and ozone (O₃) play key roles in climate change, the oxidizing capacity of the atmosphere, as well as regional and global air quality [12, 15, 16]. In recent years, spectro-radiometers in Fourier transform infrared spectroscopy (FTIS) have been widely used to monitor the concentration of atmospheric gases. An example of such spectrometer, the tropospheric emission spectrometer (TES), which is on the EOS-Aura spacecraft, was launched in July 2004 and will soon measure global three-dimensional distributions of ozone and other gases in the troposphere [3] with unprecedented accuracy. In its *nadir* mode, TES will record the spectral radiance from the Earth's atmosphere in the form of line integrals with respect to altitude z . Such measurements can be used to recover the vertical concentration profile of atmospheric gases.

Mathematically, the problem can be formulated as a one-dimensional inverse source problem of a scattering-free transport equation aiming at reconstructing the altitude-dependent gas distribution profiles [5, 7, 13] from wavenumber-dependent boundary radiation measurements. While a lot of work has been done on developing numerical algorithms to address the linear inverse problem [7, 9, 18, 20], comparatively little is known in the literature on more mathematical questions such as uniqueness and stability of the reconstruction. The first part of the paper addresses this issue.

Under suitable separability assumptions on the absorption coefficients in the transport equation, we show that the gas concentrations can indeed uniquely be determined by radiation measurements—a theoretical underpinning for the reconstruction algorithms we were not able to find in the existing literature—and give an explicit reconstruction procedure. Moreover, we stress that the reconstruction involves the inversion of a Laplace transform, which is known to be a severely ill-posed problem [4, 10, 14]. As a consequence, a somewhat limited amount of information on the profiles can be retrieved from the radiation measurements. Such limitations need to be incorporated in realistic reconstruction methods.

An important objective of the radiation measurements is the detection of relatively thin (on the order of 2–3 km) layers such as ozone or dust layers in the Earth’s lower atmosphere (the troposphere). Such layers have an important impact on local climate changes and global warming effects to cite a few. Because of the severely ill-posed nature of the inversion problem, such thin layers must be modelled specifically in the inverse problem if they are to be detected. We propose in this paper to *model* such structures as thin inclusions with arbitrary (i.e., not necessarily small) concentration contrast. We perform asymptotic expansions in the thickness of the inclusions to characterize their main impact on the boundary measurements. The technique follows general principles that have been used successfully in many other fields [1, 2, 6]. The results of the analysis are the following. The location of the inclusions and the product of their thickness and their concentration variations (with respect to the underlying medium assumed to be *known*) can be reconstructed from moderately noisy data (see simulations below). Obtaining more on the inclusion, i.e., both its thickness and its concentration, requires much more accurate data. This provides us with some guidelines in our aim to understand what can versus what cannot be reconstructed from measurements with a given noise level.

Let us note that the *nadir* measurements represent only one modality of TES. Measurements involving directions of incidence other than vertical, e.g., horizontal or *limb* sounding, provide additional information and could be incorporated into the model to improve its stability properties. Although this is an important problem, it is not considered further here.

The rest of the paper is organized as follows. Section 2 recalls the pertaining mathematical equations and the radiative transfer inverse problem. Section 3 presents a simplified model for the retrieval problem. In that setting, uniqueness and severe ill-posedness of the reconstruction are shown. The single-gas and multiple-gas cases are considered separately. Section 4 is devoted to asymptotic analyses showing the asymptotic effect on the measurements of localized anomalies with sizeable concentration variations. Several numerical simulations based on synthetic data are provided in section 5. Section 6 offers some concluding remarks.

2. Mathematical model

We denote by $L(z, \nu)$ the radiation intensity of atmospheric gases at altitude $z \in \mathcal{Z} = (0, Z)$, where Z is the altitude at the ‘top’ of the atmosphere, and wavenumber $\nu \in \mathcal{N} = [\nu_{\min}, \nu_{\max}]$, where ν_{\min} and ν_{\max} are the minimum and maximum wavenumbers accessible in real measurements. The radiation source term at the Earth surface is $L(z = 0, \nu)$. The volume

source term of radiation is $a(z, \nu)B(z, \nu)$, where $a(z, \nu)$ is the absorption profile of a specific gas in the atmosphere and $B(z, \nu)$ is the Planck function of black-body radiation. The measurements $L(Z, \nu)$ are the radiation intensity on top of the atmosphere $z = Z$. Typically, measurements are available in the wavenumber range of 650 to 2250 cm^{-1} (which corresponds to wavelengths of 15.4 and 4.4 μm , respectively). Thus, ν is in the middle of the thermal infrared region (IR). From the atmospheric radiative transfer theory [12, 15], the transport equation satisfied by $L(z, \nu)$ is

$$\begin{cases} \frac{\partial L(z, \nu)}{\partial z} + a(z, \nu)L(z, \nu) = a(z, \nu)B(z, \nu), & (z, \nu) \in \mathcal{Z} \times \mathcal{N}, \\ L(0, \nu) = L_0(\nu), & \nu \in \mathcal{N}. \end{cases} \quad (1)$$

We assume that $a(z, \nu)$ and $B(z, \nu)$ are positive functions of class $C^0(\mathcal{Z} \times \mathcal{N})$ and $C^1(\mathcal{Z} \times \mathcal{N})$, respectively, and that $L_0(\nu)$ is a positive function of class $C^0(\mathcal{N})$. As usual C^0 is the class of continuous functions and C^1 the class of continuously differentiable functions. The solution $L(z, \nu)$ is then a positive function of class $C^1(\mathcal{Z} \times \mathcal{N})$ [11].

The Planck function $B(z, \nu)$ is given by

$$B(z, \nu) = \frac{2h\nu^3}{c^2(e^{h\nu/kT(z)} - 1)}, \quad (2)$$

where h is Planck constant, ν is the wavenumber, k is the Boltzmann constant and c is the speed of light in a vacuum. The temperature profile $T(z)$, assumed here to be of class $C^1(\mathcal{Z})$, is given in Kelvin degrees and is thus always positive. Note however that $T'(z)$ changes sign on \mathcal{Z} in practice. This will be important in the reconstruction theory. Scattering has been neglected in (1), which is an accurate assumption in the ‘clear sky’ environment.

The radiation intensity at the Earth surface is related to the Planck constant of black-body radiation by

$$L_0(\nu) = \varepsilon(\nu)B(0, \nu) \quad (3)$$

where $\varepsilon(\nu)$ is the surface emissivity, which we may assume is constant at the Earth’s surface $\varepsilon(\nu) = \varepsilon$ [15].

It is more convenient to work in the following with the quantity

$$H(z, \nu) = L(z, \nu) - B(z, \nu), \quad (4)$$

modelling the departure from the black-body radiation equilibrium. One can verify that the equation for $H(z, \nu)$, also of class $C^1(\mathcal{Z} \times \mathcal{N})$, takes the form

$$\begin{cases} \frac{\partial H(z, \nu)}{\partial z} + a(z, \nu)H(z, \nu) = -\frac{\partial B(z, \nu)}{\partial z} \equiv S(z, \nu), & (z, \nu) \in \mathcal{Z} \times \mathcal{N}, \\ H(0, \nu) = \gamma B(0, \nu), & \nu \in \mathcal{N}, \end{cases} \quad (5)$$

where $\gamma = \varepsilon - 1$. Upon inverting this first-order ordinary differential equation, we get

$$\begin{aligned} H(Z, \nu) &= H(0, \nu) \exp\left(-\int_0^Z a(\zeta, \nu) d\zeta\right) + \int_0^Z S(\zeta, \nu) \\ &\quad \times \exp\left(-\int_\zeta^Z a(\zeta, \nu) d\zeta\right) dz, \quad \nu \in \mathcal{N}. \end{aligned} \quad (6)$$

Let us define the optical length

$$\alpha(z, \nu) = \int_z^Z a(\zeta, \nu) d\zeta. \quad (7)$$

We may then recast the above integral (6) as

$$H(Z, \nu) = H(0, \nu) e^{-\alpha(0, \nu)} + \int_0^Z S(\zeta, \nu) e^{-\alpha(z, \nu)} dz, \quad \nu \in \mathcal{N}. \quad (8)$$

This is the integral formulation, equivalent to the differential equation (1), as it appears in most of the atmospheric inversion literature.

3. Uniqueness and ill-posedness of a simplified model

We know that the absorption profile $a(z, \nu)$ depends on both the concentration of atmosphere gases and their absorption properties at specific wavenumbers. To simplify the presentation, we assume in this section that only one gas, such as ozone, contributes to absorption and emission. We then have that

$$a(z, \nu) = c(z)\kappa(z, \nu), \quad (9)$$

where $c(z) \in C^0(\mathcal{Z})$ is the unknown (non-negative) concentration profile for the gas, and $\kappa(z, \nu) \in C^0(\mathcal{Z} \times \mathcal{N})$ is the (positive) spectral absorption/emission coefficient (also called spectral line shape). Although more complicated models of $\kappa(z, \nu)$ can be considered, we focus here on the so-called Lorentzian line shape of $\kappa(z, \nu)$. It is valid in the lower atmosphere and takes the form

$$\kappa(z, \nu) \equiv \kappa_L(z, \nu) = Q_{\nu_0} \frac{1}{\pi} \frac{\alpha_L(z)}{(\nu - \nu_0)^2 + \alpha_L^2(z)} \equiv Q_{\nu_0} f(z, \nu - \nu_0), \quad (10)$$

where ν_0 is the centre of the band of wavenumber we are interested in and $Q_{\nu_0} = \int_{\mathcal{N}} \kappa(z, \nu) d\nu$ is the line strength. The function $\alpha_L \in C^0(\mathcal{Z})$ is called the Lorentz half-width. It is roughly given by

$$\alpha_L(z) \sim T(z)^{-1/2}, \quad z \in \mathcal{Z}, \quad (11)$$

where $T(z)$ is the temperature profile of the atmosphere and $f(z, \nu - \nu_0) \in C^0(\mathcal{Z} \times \mathcal{N})$ is the shape factor of a spectral line [12]. The Lorentzian line shape describes how a gas absorbs and emits radiance in a narrow band of wavenumbers centred at ν_0 .

The inverse (retrieval) problem in atmosphere imaging is to assume that the radiation term $B(z, \nu)$ in (1) and absorption coefficient $\kappa(z, \nu)$ are known and to reconstruct as much as possible about $c(z)$ from radiation measurements $L(Z, \nu) = H(Z, \nu) + B(Z, \nu)$.

3.1. The case of a single gas

The purpose of this section is to show that the reconstruction of $c(z)$ from $L(Z, \nu)$ is uniquely determined (in a slightly simplified setting) and is a *severely ill-posed* problem (see [10]) in the sense that, in the absence of regularization, noise in the data is more amplified during the inversion procedure than what would result from an arbitrary number of differentiations.

We do not have a complete theory for general absorption coefficient $\kappa(z, \nu)$. Rather we make the following *assumption* on the shape factor $f(z, \nu - \nu_0)$:

$$f(z, \nu - \nu_0) = \mu(\nu - \nu_0)g(z), \quad (12)$$

where $g(z) \in C^0(\mathcal{Z})$ is uniformly bounded from below by a positive constant, and $\mu(\nu - \nu_0) \in C^0(\mathcal{N})$ is a positive function whose range $\mathcal{M} = \mu(\mathcal{N} - \nu_0)$ is an interval in \mathbb{R}^+ . In the above expression (10) this would correspond to replacing κ by its approximation

$$\kappa_L(z, \nu) \approx Q_{\nu_0} \frac{1}{\pi} \frac{\alpha_L(z)}{(\nu - \nu_0)^2 + \bar{\alpha}^2}, \quad (13)$$

with $\mu(\nu)$ and $g(z)$ given by

$$\mu(\nu) = \frac{1}{\pi} \frac{\bar{\alpha}}{\nu^2 + \bar{\alpha}^2}, \quad (14)$$

and

$$g(z) = \frac{\alpha_L(z)}{\bar{\alpha}}. \quad (15)$$

Here $\bar{\alpha}$ is a constant. The range of μ is given by $\mathcal{M} = \left[\frac{\bar{\alpha}}{\pi(\bar{\nu}^2 + \bar{\alpha}^2)}, \frac{1}{\pi\bar{\alpha}} \right] \subset \mathbb{R}^+$ with $\bar{\nu} := \max(|\nu_{\min} - \nu_0|, |\nu_{\max} - \nu_0|)$.

The separability assumption on the shape factor is not totally unreasonable for the Lorentzian line shape (10). Following (11) and choosing $\bar{\alpha} \sim \bar{T}^{-1/2}$, where \bar{T} the average of $T(z)$ over \mathcal{Z} , we obtain from realistic temperature profiles that $\left\| \frac{\alpha_L - \bar{\alpha}}{\alpha_L} \right\|_{L^\infty(\mathcal{Z})} < 0.15$, which implies that at any given wavenumber ν , $\left\| \frac{\kappa(\cdot, \nu) - \kappa_L(\cdot, \nu)}{\kappa(\cdot, \nu)} \right\|_{L^\infty(\mathcal{Z})} < 0.15$, where κ and κ_L are given by (10) and (13), respectively. The maximal error is attained when $\nu = \nu_0$ and decays quite fast away from ν_0 because of the dominance of the term $(\nu - \nu_0)^2$ over α_L^2 . Therefore, the separability assumption serves as a faithful benchmark in understanding the theoretical and numerical aspects of reconstructions based on more detailed and accurate physical models.

We also simplify the behaviour of the source terms with respect to wavenumber ν and approximate the Planck function (2) as follows:

$$B(z, \nu) \approx \frac{2k\nu^2}{c^2} T(z). \quad (16)$$

We verify that in the infrared region of interest, this expansion is quite accurate as $h\nu/kT$ is on the order of at most 10^{-3} in practice. The temperature $T(z)$ is also assumed to be of class $C^1(\mathcal{Z})$.

Accounting for the above simplifications and using the change of variables $\nu \rightarrow \mu$ and $H(z, \nu)c^2/(2k\nu^2) \rightarrow D(z, \mu)$, we obtain, still denoting by $a(z, \mu)$ and $\kappa(z, \mu)$ the absorption coefficients in the new variables, that $D(z, \mu)$ satisfies the following equation:

$$\begin{cases} \frac{\partial D(z, \mu)}{\partial z} + a(z, \mu)D(z, \mu) = -\frac{\partial T(z)}{\partial z} \equiv S(z), & (z, \mu) \in \mathcal{Z} \times \mathcal{M}, \\ D(0, \mu) = \gamma T(0), & \mu \in \mathcal{M}. \end{cases} \quad (17)$$

After defining the *rescaled* optical length by

$$\alpha(z) = \int_z^Z Q_{\nu_0} c(\zeta) g(\zeta) d\zeta, \quad (18)$$

equation (17) can be inverted as

$$D(Z, \mu) = D(0) e^{-\mu\alpha(0)} + \int_0^Z S(z) e^{-\mu\alpha(z)} dz, \quad \mu \in \mathcal{M}. \quad (19)$$

Here $D(Z, \mu)$ is the measurement for $\mu \in \mathcal{M}$. The positive function $g(z)$ and the temperature profile $T(z)$ (hence $S(z)$) are *known a priori*.

The inverse problem for (17) is then:

(IP) Determine the positive function $c(z) \in C^0(\mathcal{Z})$ from the measurements $D_m(\mu) = D(Z, \mu)$ for $\mu \in \mathcal{M}$.

As we have already mentioned, several numerical methods have been devised for solving the above inverse problem; see [7, 9, 20] and the monograph [18] and references therein. Many techniques are based on Bayesian inversion techniques [9, 18]. In this paper we concentrate on the mathematical analysis of the continuous (non-discretized) inverse problem (IP). Our main result is the following:

Theorem 3.1. *Let us assume that $S(z)$ is a continuous function on \mathcal{Z} , which vanishes at a finite (possibly zero) number of points. Then there is a unique strictly positive function $c(z) \in C^0(\mathcal{Z})$ solving (IP).*

Proof. The gas concentration profile $c(z)$ and the quantity $g(z)$ in (15) are both positive functions on $\mathcal{Z} = (0, Z)$, so $\alpha'(z) = -Q_{v_0}c(z)g(z) < 0$ on \mathcal{Z} . We can then perform the change of variables $z \mapsto \alpha(z)$ and define the continuously differentiable inverse map $\alpha \mapsto z(\alpha)$. The above inequality implies that $z'(\alpha) < 0$. The transform (19) may thus be recast as

$$D(Z, \mu) = D(0) e^{-\mu\alpha(0)} + \int_0^{\alpha(0)} S(z(\alpha)) \left| \frac{dz}{d\alpha} \right| e^{-\mu\alpha} d\alpha, \quad \mu \in \mathcal{M}. \quad (20)$$

Here we have used that $\alpha(Z) = 0$. The data $D(Z, \mu)$ are thus the *Laplace transform* of the distribution

$$h(\alpha) \equiv -z'(\alpha)S(z(\alpha)) + D(0)\delta(\alpha - \alpha(0)). \quad (21)$$

The above distribution has support in $[0, \alpha(0)]$. Since it is compactly supported, its Fourier transform $\hat{h}(\zeta) = \frac{1}{2\pi} \int_{\mathbb{R}} e^{i\zeta\alpha} h(\alpha) d\alpha$ is an analytic function in ζ [23]. The latter is known for values of ζ such that $\zeta = i\mu, \mu \in \mathcal{M}$ since then $D(Z, \mu) = \hat{h}(-i\zeta)$. It is thus sufficient to know $D(Z, \mu)$ on a set with at least one accumulation point to uniquely define $\hat{h}(\zeta)$ for all $\zeta \in \mathbb{C}$ by analytic continuation [8, 19]. This in turn uniquely defines the function $h(\alpha)$. Since \mathcal{M} is an interval in our model, we can thus reconstruct $\alpha(0)$, $D(0)$ and $-z'(\alpha)S(z(\alpha))$ on $(0, \alpha(0))$ from the measurements $D(Z, \mu)$.

We now reconstruct $\alpha(z)$ on $(0, Z)$ from the above measurements. We present two similar methods. Let us first introduce the function $\tilde{T}(\alpha)$ of class $C^1(0, \alpha(0))$ defined by $\tilde{T}(\alpha) = T(z(\alpha))$. We verify that $-z'(\alpha)S(z(\alpha)) = \tilde{T}'(\alpha)$. By integration, and since $\tilde{T}(0) = T(Z)$ is known, we uniquely reconstruct $\tilde{T}(\alpha)$ on $(0, \alpha(0))$. Since $z'(\alpha) < 0$, we deduce that $\tilde{T}'(\alpha) = T'(z(\alpha))z'(\alpha)$ and $T'(z)$ vanish at the same singular points (in their respective variables). If there is no such point, then $T(z)$ is a homeomorphism on $(0, Z)$ (it is bijective, continuous, and maps open sets to open sets since $|T'(z)| > 0$ on the interval; it thus admits a continuous inverse) with inverse $z(T)$, from which we deduce $z(\alpha) = z(\tilde{T}(\alpha))$ on $(0, Z)$; whence its inverse $\alpha(z)$. Otherwise, we call the singular points α_k and $z_k, 1 \leq k \leq N$, respectively, with $\alpha(z_k) = \alpha_k$. We also note the endpoints $\alpha_0 = 0, \alpha_{N+1} = \alpha(0), z_0 = Z$ and $z_{N+1} = 0$. The points α_k are determined by the data since $\tilde{T}(\alpha)$ is known, and the points z_k are determined by knowledge of $T(z)$. On each interval $(z_{j+1}, z_j), T(z)$ is a homeomorphism with inverse function $z(T)$ (for the same reasons as above). We thus obtain $z(\alpha) = z(\tilde{T}(\alpha))$ on (z_{j+1}, z_j) , whence $\alpha(z)$ on (α_j, α_{j+1}) . Varying $0 \leq j \leq N$, this allows us to reconstruct $\alpha(z)$ on the whole interval $(0, Z)$.

Another (very similar) way of looking at the reconstruction is to recast (21) for $z \in \mathcal{Z}$ as

$$\frac{dz(\alpha)}{d\alpha} = -\frac{h(\alpha)}{S(z(\alpha))}. \quad (22)$$

The above (nonlinear) ordinary differential equation for $z(\alpha)$ holds at all but possibly a finite number of points in \mathcal{Z} by assumption on $S(z)$ and can be extended by continuity to the whole interval since $z(\alpha)$ is a C^1 diffeomorphism. We thus uniquely recover the diffeomorphism $z(\alpha)$ from (22) since $h(\alpha)$ is continuous on $(0, \alpha(0))$ as can be seen in (21) and provided that $S(z)$ is a Lipschitz function (hence the above ordinary differential equation admits a unique solution; this proof requires a little more regularity than the previous one). This also uniquely defines its inverse $\alpha(z)$. Once α is reconstructed we uniquely reconstruct $c(z)$ by differentiating formula (18). This complete the proof. \square

Both the analytic continuation [17] and the inversion of the Laplace transform [4] are known to be *severely ill-posed* problems. The reconstruction of the concentration profiles from the boundary measurements is therefore severely ill-posed, even if we had access to data

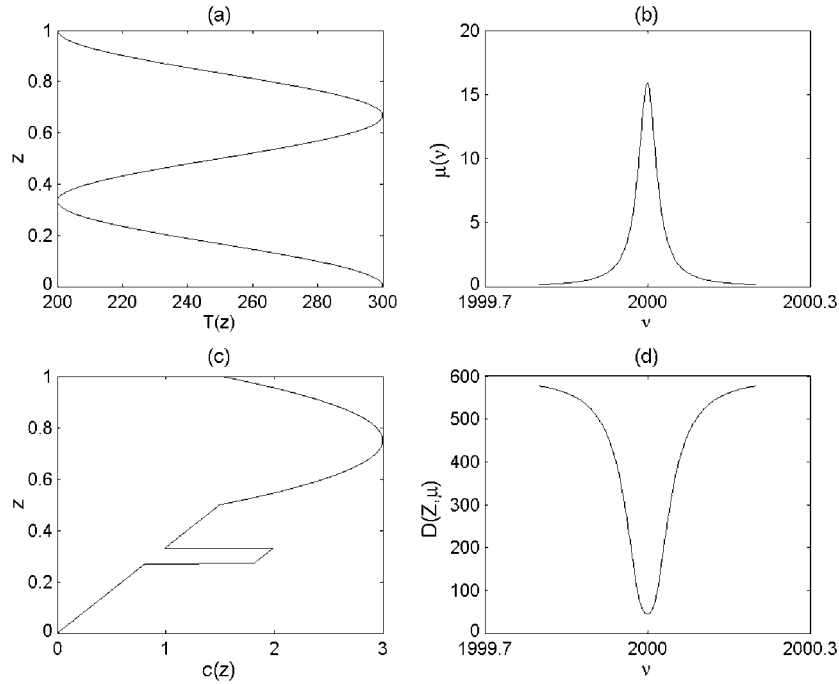


Figure 1. Profiles used in the calculation. (a) Temperature profile as a function of z . (b) Rescaled absorption as a function of wavelength. (c) Ozone concentration as a function of z . (d) Data $D(Z, \mu(v))$ as a function of wavenumber v .

on $\mathcal{M} = \mathbb{R}^+$ (in which case the reconstruction would still rely on inverting a Laplace transform). In practice, this means that only a handful of parameters modelling the concentration profile can realistically be reconstructed from the measured data provided that those data contain only high-frequency noise.

The assumption that the temperature gradient $S(z)$ may vanish at a finite number of points allows us to account for non-invertible temperature profiles (i.e., $z(T)$ may be a multi-valued function; the assumption on $S(z)$ implies that it can only take a finite number of values). The temperature profiles are not invertible in practice, see figure 1(a), so we need to account for this situation. The assumption however cannot be substantially relaxed. If $S(z)$ vanishes on an interval, then $\alpha'(z)$ cannot be reconstructed on this interval since (21) and (22) are no longer equivalent. The measurements at $z = Z$ provide no information on $\alpha(z)$ on the intervals where $S(z)$ vanishes. This implies non-uniqueness of the gas profile reconstruction; see also our numerical simulation at the end of section 5.1.

3.2. The case of multiple gases

We now extend the results obtained in the preceding section to the multiple-gas case. Let us assume that our composite gas consist of M different species and the absorption spectra of the composite gas contain N ($N \geq M$) well-separated bands centred at v_i , $i = 1, 2, \dots, N$, respectively. By ‘well-separated’ we mean that for wavenumbers v in the j th band, we have $|v - v_j| \ll |v_k - v_j|$, for all $k \neq j$. We assume moreover that the absorption coefficient for gas i can be written as

$$\kappa_i(z, v) = Q_{ij} \mu(v - v_j) c_i(z) g_i(z), \quad (23)$$

where Q_{ij} is the line intensity for gas i in the wavenumber band j . Our main assumption is that the function $\mu(v)$ with range \mathcal{M} is universal to all gases and takes the form (14), i.e.,

$$\mu(v) = \frac{1}{\pi} \frac{\bar{\alpha}}{v^2 + \bar{\alpha}^2}, \quad (24)$$

where $\bar{\alpha}$ is a constant. With these assumptions we have the following (relatively straightforward) generalization of the single gas case:

Theorem 3.2. *Under the assumptions of theorem 3.1, there exists a unique set of positive profiles $c_i(z)$, $i = 1, \dots, M$, such that $D(Z, \mu) \equiv D_m(Z, \mu)$ provided that assumptions (23) and (24) hold and the matrix Q_{ij} has rank M .*

Proof. With the above assumptions, we can write the total absorption map for the composite gas in the vicinity of band j as

$$a(z, v) \equiv a_j(z, v) = \mu(v - v_j) \sum_{i=1}^M Q_{ij} c_i(z) g_i(z). \quad (25)$$

After defining

$$\alpha_j = \sum_{i=1}^M Q_{ij} \int_z^Z c_i(\zeta) g_i(\zeta) d\zeta, \quad (26)$$

we obtain a similar expression as before for the measurements $D_j(Z, \mu)$ in the j th frequency band:

$$D_j(Z, \mu) = D(0) e^{-\mu\alpha_j(0)} + \int_0^Z S(z) e^{-\mu\alpha_j(z)} dz. \quad (27)$$

For the same reason as in one gas case, since $\alpha_j' < 0$, we can perform the change of variables $z \rightarrow \alpha_j(z)$. Defining the inverse map $\alpha_j \mapsto z(\alpha_j)$, we obtain

$$D_j(Z, \mu) = D(0) e^{-\mu\alpha_j(0)} + \int_0^{\alpha_j(0)} S(z(\alpha_j)) \left| \frac{dz}{d\alpha_j} \right| e^{-\mu\alpha_j} d\alpha_j. \quad (28)$$

We can thus regard $D(Z, \mu)$ as the *Laplace transform* of the distribution

$$h(\alpha_j) \equiv D(0)\delta(\alpha_j - \alpha_j(0)) + S(z(\alpha_j)) \left| \frac{dz}{d\alpha_j} \right|. \quad (29)$$

Then, by the same argument as in the single gas case, we can uniquely reconstruct $\alpha_j(z)$. According to (26), we can uniquely recover

$$\sum_{i=1}^M Q_{ij} c_i(z) g_i(z) = \alpha_j'(z), \quad j = 1, \dots, N. \quad (30)$$

The above inversion can be performed in each of the N absorption bands, after which we arrive at the following system of equations for $c_i(z) g_i(z)$:

$$\begin{pmatrix} Q_{11} & \cdots & Q_{1M} \\ \vdots & \ddots & \vdots \\ Q_{N1} & \cdots & Q_{NM} \end{pmatrix} \begin{pmatrix} c_1 g_1 \\ \vdots \\ c_M g_M \end{pmatrix} (z) = \begin{pmatrix} \alpha_1' \\ \vdots \\ \alpha_N' \end{pmatrix} (z). \quad (31)$$

Since the matrix (Q_{ij}) has rank M , the above system admits at most one solution, is invertible when $M = N$, and provides the unique solution if the source terms $\alpha_j'(z)$ are compatible. This implies that we can uniquely determine the concentration profiles $c_i(z)$ from the measured data and concludes the proof. \square

In many practical situations, the matrix (Q_{ij}) is indeed invertible (with $N = M$). Such examples can be seen in [16], where it appears that the matrix Q is often diagonally dominant. A diagonally dominant square matrix, i.e., such that $|Q_{ii}| > \sum_{j \neq i}^M |Q_{ij}|$ for all $i = 1, \dots, M$, is known to be invertible [21].

4. Small inclusions

We have seen in earlier sections that the reconstruction of concentration profiles from radiation measurements was a severely ill-posed problem. This implies that only very few coefficients parametrizing the concentration can be reconstructed from the measurements provided that noises contained in data have only high-frequency components. Therefore localized inclusions such as ozone or dust layers, whose detection is important in many applications, may be poorly reconstructed unless their presence is explicitly parametrized.

We proposed here to model such layers as localized inclusions of small thickness and arbitrary concentration variations compared to the underlying medium that will be assumed to be *known*. The problem of reconstructing localized diffusive or absorbing inhomogeneities has been extensively studied in medical imaging problems [1, 2, 6]. We now consider such a model in profile retrieval and carry out a similar analysis.

4.1. The case of a single gas

Let us start with the case of a single inclusion composed of a single gas. We assume that the background profile $c_0(z)$ is known. The true profile is given by

$$c(z) = c_0(z) + \delta c(z). \quad (32)$$

The assumption on $\delta c(z)$ is *not* that it is small in $L^\infty(\mathcal{Z})$ but rather that it is small in $L^1(\mathcal{Z})$ and of ‘small’ support. We assume that $\delta c(z)$ takes the (arbitrarily large) value δc on an interval centred at $z = z_0$ and of size δz and takes the value 0 elsewhere:

$$\delta c(z) = \delta c \chi_{I_z}(z), \quad I_z = \left[z_0 - \frac{\delta z}{2}, z_0 + \frac{\delta z}{2} \right].$$

Here, $\chi_{I_z}(z)$ is the indicatrix function of the interval I_z .

Let us denote by $\alpha_0(z)$ the optical length corresponding to the background profile c_0 only. We then observe from equation (19) that

$$\begin{aligned} D[c_0 + \delta c](Z, \mu) &= D(0) \exp(-\mu \alpha_0(0)) \exp\left(-\mu \delta c \int_{I_z} g(\zeta) d\zeta\right) \\ &+ \int_0^Z S(z) \exp(-\mu \alpha_0(z)) \exp\left(-\mu \delta c \int_{I_z \cap (z, Z)} g(\zeta) d\zeta\right) dz. \end{aligned} \quad (33)$$

By hypothesis, $D[c_0](Z, \mu)$ is known and we thus have access by approximating $D[c_0 + \delta c](Z, \mu) - D[c_0](Z, \mu)$, to first order in δz , to the following quantity:

$$\mu \mapsto \mu \delta c \delta z g(z_0) \left[D(0) e^{-\mu \alpha_0(0)} + \int_0^{z_0} S(z) e^{-\mu \alpha_0(z)} dz \right]. \quad (34)$$

Taking the ratio at two different values of μ gives a functional $\mathcal{F}(z_0)$. It is straightforward to check that $z_0 \mapsto \mathcal{F}(z_0)$ is a smooth function. On each interval such that $\mathcal{F}'(z_0) \neq 0$ we can thus uniquely reconstruct z_0 in a stable way. In practical applications, $\mathcal{F}'(z_0)$ may vanish at a finite number of points so that the function $\mathcal{F}(z_0)$ is not monotone. The point z_0 is then not uniquely reconstructed. However it can be uniquely reconstructed when we know *a priori* on

which interval z_0 belongs where $\mathcal{F}(z_0)$ does not vanish. Once z_0 is known, we easily obtain $\delta c \delta z$ from the above expression.

Consequently, provided that we have a sufficiently accurate knowledge of the background and that the term $\delta c \delta z$ is sufficiently small, we can reconstruct in a stable way the location of the inclusion z_0 and $\delta c \delta z$, which for want of a better word we will call its *strength*. Moreover this can ideally be performed from only two measurements corresponding to two different values of μ .

We now verify by asymptotic expansions that the first term allowing us to separate δz from δc is of order δz^3 . Indeed, upon carrying out a higher order Taylor expansion in (33) we deduce that

$$D[c_0 + \delta c](Z, \mu) - D[c_0](Z, \mu) = \left(-\mu \delta c \delta z g_0 + \frac{1}{2} \mu^2 g_0^2 \delta c^2 \delta z^2 - \frac{1}{6} (\mu g_0'' \delta c + \mu^3 g_0^3 \delta c^3) \delta z^3 \right) \times \left[D(0) e^{-\mu \alpha_0(0)} + \int_0^{z_0} S(z) e^{-\mu \alpha_0(z)} dz \right] + O(\delta z^4), \quad (35)$$

where $g_0 = g(z_0)$ and $g_0'' = g''(z_0)$.

So when the noise in the data is of order $O(\delta z^4)$ or higher, we can reconstruct z_0 , δz and δc as we have access to $\delta c \delta z^3$ in the term of order $O(\delta z^3)$, at least provided that $g''(z_0)$ does not vanish. However when the noise in the data is of order $O(\delta z^3)$ or larger, all we can possibly reconstruct from the measurements is the location z_0 and the product $\delta c \delta z$. This corresponds to knowing the total amount of ozone variation in the layer but not the respective thickness and concentration variation. If the noise in the data is larger than $\delta c \delta z$, then even this information cannot be retrieved unless a more careful statistical model is considered.

We now consider a case where the location z_0 cannot be recovered uniquely. We deduce from (34) that all the information we have access to about z_0 is contained in $g(z_0) \left(D(0) e^{-\mu \alpha_0(0)} + \int_0^{z_0} S(z) e^{-\mu \alpha_0(z)} dz \right) \equiv G(z_0)$. Both $g(z)$ and $S(z)$ are related to the temperature profile $T(z)$. Suppose that $T(z)$ is constant on an interval I so that $S(z)$ vanishes on I . Then we verify that $G(z)$ is constant on I , which means that z_0 cannot be reconstructed uniquely when the inclusion is located in a region of constant temperature. Note that the hypotheses of theorem 3.1 are not satisfied in this case. Consequently, if one tries to recover z_0 by a gradient-based optimization technique such as a Newton or conjugate gradient (CG) method [22], the gradient of objective functional (for instance $\mathcal{F}(z_0)$) with respect to z_0 will vanish for $z_0 \in I$; see the numerical simulations in section 5.

4.2. The case of multiple gases

Let us now briefly extend the analysis in the case of M gases assuming the existence of M (to simplify) separated wavenumber bands as described in (23). The asymptotic analysis is based on formula (27). As in the single-gas case, we assume that the profile for each gas is a superposition of a known background and localized variations of arbitrary contrast. More precisely, we have

$$c_i(z) = c_{0i}(z) + \delta c_i(z), \quad i = 1, \dots, M, \quad (36)$$

where c_{0i} is the background concentration profile for species i and where the fluctuations are modelled by

$$\delta c_i(z) = \delta c_i \chi_{I_i}(z), \quad I_i = \left[z_i - \frac{\delta z_i}{2}, z_i + \frac{\delta z_i}{2} \right], \quad i = 1, \dots, M.$$

As before, $\chi_{I_{z_i}}(z)$ is the indicatrix function of the interval I_{z_i} . We assume also that all thicknesses δz_i are of the same order $O(\delta z)$. We assume here that each gas may have strong fluctuations in only one layer. The generalization to multiple layers is straightforward and is not considered. This may be accounted for in the present theory by stipulating that several indices $1 \leq j \leq M$ correspond to the same gas.

Upon inserting the above approximation into formula (27), we obtain

$$D[c_{01} + \delta c_1, \dots, c_{0M} + \delta c_M](Z, \mu) = D(0) \exp(-\mu \alpha_j^0(z)) \exp\left(-\mu \sum_i^M Q_{ij} \delta c_i \int_{I_{z_i}} g(\zeta) d\zeta\right) \\ + \int_0^Z S(z) \exp(-\mu \alpha_j^0(z)) \exp\left(-\mu \sum_i^M Q_{ij} \delta c_i \int_{I_{z_i} \cap (z, Z)} g(\zeta) d\zeta\right) dz, \quad (37)$$

where α_j^0 denotes the optical length α_j in (26) defined with the background profile. Upon performing a second-order Taylor expansion in the above formula, we get

$$D_j[c_{01} + \delta c_1, \dots, c_{0M} + \delta c_M](Z, \mu) - D_j[c_{01}, \dots, c_{0M}](Z, \mu) \\ = -\mu \sum_{i=1}^M (Q_{ij} \delta c_i \delta z_i g_i(z_i) \bar{S}(\mu, z_i)) + \mu^2 \sum_{i=1}^M (Q_{ij} \delta c_i \delta z_i g_i(z_i))^2 \bar{S}(\mu, z_i) \\ + \mu^2 \sum_{i=1}^M \sum_{i \neq k=1}^M Q_{ij} \delta c_i \delta z_i g_i(z_i) Q_{kj} \delta c_k \delta z_k g_k(z_k) \bar{S}(\mu, \min(z_i, z_k)) + O(\delta z^3), \quad (38)$$

where we have defined the averaged source term

$$\bar{S}(\mu, z_i) \equiv \int_0^{z_i} S(z) e^{-\mu \alpha_j^0(z)} dz + D(0) e^{-\mu \alpha_j^0(0)}. \quad (39)$$

Higher order terms can be obtained similarly although their expression becomes much more cumbersome. Note that we recover (34) when $M = 1$. Suppose that the error in the measured data is of order $O(\delta z^2)$. Then we only have access to the information

$$\mu \mapsto \mu \sum_{i=1}^M Q_{ij} \delta c_i \delta z_i g_i(z_i) \bar{S}(\mu, z_i). \quad (40)$$

Assuming that the matrix $(Q_{ij})_{i,j}$ is a square invertible matrix, we can reconstruct from measurements in M well-separated bands the quantities defined by

$$p_i \equiv \mu \delta c_i \delta z_i g_i \bar{S}(\mu, z_i). \quad (41)$$

This information has the same structure as in the single-gas case. From a minimum of two measurements, we can reconstruct the location z_i . An accuracy of order $O(\delta z)$ in the data then allows us to reconstruct the strength of the i th inclusion $\delta c_i \delta z_i$. The same products appear in the terms proportional to δz^2 . Therefore an accuracy in the data of order $O(\delta z^3)$ is again necessary to estimate δz_i and δc_i separately.

5. Numerical reconstructions

We present in this section several numerical simulations that illustrate the theory developed in the preceding section. The atmosphere thickness is normalized to $Z = 1$. We first concentrate on the single-gas case and then consider an example with a mixture of two gases. All the data are synthetic and the cases considered academic. However, we have chosen temperature and concentration profiles that are qualitatively very similar to those analysed in [5].

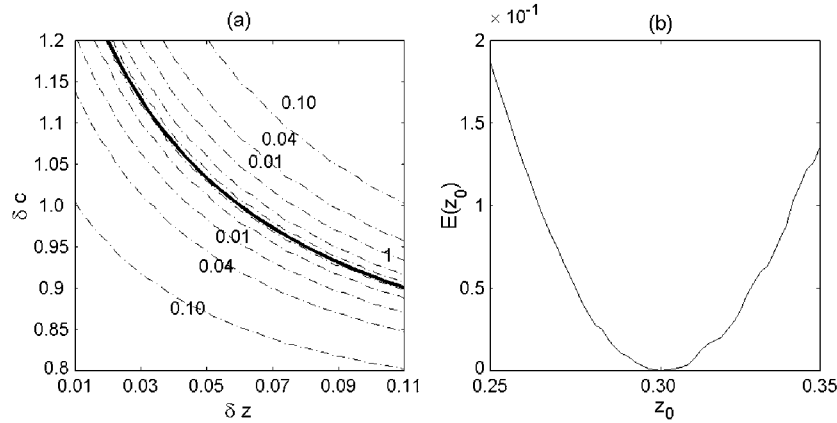


Figure 2. Cross section of the error functional in the parameter space. (a) Functional at $z_0 = 0.3$; (b) functional at $\delta z = 0.06$ and $\delta c = 1.0$.

5.1. The case of a single gas

We start with the single-gas model. We illustrate the predictions of the asymptotic expansions that different properties of the localized inclusions can be retrieved from the measured data depending on the noise level. The concentration profile is given by

$$c_0(z) = \begin{cases} 3z & z \in (0, 0.5] \\ 3.0 - 20(z - 0.75)^2 & z \in (0.5, 1.0), \end{cases} \quad (42)$$

which is a simplified model for the concentration profile of ozone in the atmosphere below 40 km. A thin inclusion is located at $z_0 = 0.3$. The characteristics of that inclusion are that $\delta z = 0.06$ and $\delta c = 1.0$. The temperature profile is modelled by

$$T(z) = 250 + 50 \sin\left(3\pi z + \frac{\pi}{2}\right), \quad z \in (0, 1), \quad (43)$$

which qualitatively resembles the observed profiles. Figure 1 shows the concentration profile, the temperature distribution, the absorption line shape used in the calculations and the solution of equation (17) with respect to wavenumber ν .

The location and characteristics of the inclusion are reconstructed by two methods. In the first method, we minimize the error of the forward model to the true data by using a full search algorithm. This can be done because only three parameters need to be recovered in this case. More precisely we search on a $101 \times 101 \times 401$ uniformly distributed mesh for $(z_0, \delta z, \delta c)$ in the parameter space $[0.25, 0.35] \times [0.01, 0.11] \times [0.80, 1.20]$. We look for the minimum of the least-square error functional

$$E(z_0, \delta z, \delta c) = \int_{\mathcal{M}} (D(Z, \mu) - D_m(\mu))^2 d\mu, \quad (44)$$

where $D_m(\mu)$ represents the measurement data. In the numerical simulations, we take $Q_0 = \bar{\alpha} = 2 \times 10^{-2}$, $\mathcal{M} = \frac{1}{\pi} \left[\frac{1}{101}, 1 \right]$, which means that the wavenumbers either belong to $[1999.8, 2000]$ or to $[2000, 2000.2]$ by symmetry. We use 200 wavenumbers in each band.

We show in figure 2 the distribution of the error in parameter space. In figure 2(a), we present the function at $z_0 = 0.3$ (dashed lines), and the function at $z_0 = 0.3$ and $\delta z \delta c = 0.06$ (thick solid line). We observe that the functional varies quite substantially in the direction of increase (or decrease) of $\delta z \delta c$ but remains almost constant in the orthogonal direction (i.e.,

Table 1. Characteristics of the inclusion reconstructed by a full search algorithm. The true values are $z_0 = 0.3$, $\delta z = 0.06$, $\delta c = 1.0$, hence $\delta z \delta c = 0.06$. The numbers in parentheses denote the relative error in percentage between the reconstructed parameters and their true values.

Noise	z_0 (error in %)	δz (error in %)	δc (error in %)	$\delta z \delta c$ (error in %)
0.00%	0.3000 (0.0)	0.0600 (0.0)	1.0000 (0.0)	0.0600 (0.0)
0.05%	0.3000 (0.0)	0.0590 (1.7)	1.0180 (1.8)	0.0597 (0.5)
0.10%	0.2970 (1.0)	0.0570 (6.0)	1.0430 (4.3)	0.0592 (1.4)
1.00%	0.2950 (1.7)	0.0490 (18.0)	1.1870 (18.0)	0.0581 (3.1)

Table 2. Same as table 1 (with the *same* noisy measurements) except that the conjugate gradient algorithm is used in the optimization process.

Noise	z_0 (error in %)	δz (error in %)	δc (error in %)	$\delta z \delta c$ (error in %)
0.00%	0.3000 (0.0)	0.0600 (0.0)	1.0000 (0.0)	0.0601 (0.2)
0.05%	0.3000 (0.0)	0.0591 (1.7)	1.0177 (1.8)	0.0602 (0.3)
0.10%	0.2971 (1.0)	0.0572 (4.7)	1.0386 (3.9)	0.0594 (1.0)
1.00%	0.2952 (1.6)	0.0492 (18.0)	1.1811 (18.0)	0.0581 (3.1)

along curves where $\delta z \delta c$ is constant). Finding the curve where $\delta c \delta z$ is minimal can thus be achieved even with quite substantial noise in the data. Finding the global minimum of the functional, which is necessary to separately reconstruct δc and δz , requires much more accurate data. Figure 2(b) shows that the functional with respect to z_0 , the location of the inclusion, at δc and δz fixed to their exact value, is quite well behaved. This indicates that z_0 can also be reconstructed in quite a stable way.

Table 1 lists the parameters recovered by the full search algorithm. The accuracy in the recovery of δz and δc decreases as the noise level increases. The location of the inclusion z_0 and the product $\delta z \delta c$ can be obtained satisfactorily even with a relatively high-noise level of around 1%. However, at this level of noise, the reconstruction of δz and δc is no longer reliable with relative errors as high as 20%. In all our simulations, a noise level of $x\%$ means that a uniformly distributed random number between $-x\%$ and $x\%$ has been added.

As the number of parameters increases, full search algorithms are not tractable. We have repeated the preceding reconstruction by using the conjugate gradient method [22] to minimize the least-squares-error functional (44),

$$\min_{z_0, \delta z, \delta c} E. \quad (45)$$

The initial guess for the parameters are $z_0 = 0.27$, $\delta z = 0.07$ and $\delta c = 1.2$. The results are list in table 2 and are very similar to those obtained with the full search algorithm. The CG algorithm was found to be relatively robust with respect to the choice of the initial guess.

Let us now consider the special case where uniqueness in the reconstruction of z_0 is not guaranteed. This happens when the temperature gradient vanishes on an interval \mathcal{I} including the inclusion's location. The temperature profile is now chosen to be

$$T(z) = \begin{cases} 250 + 50 \sin(3\pi z + \frac{\pi}{2}) & z \in (0, 0.1) \cup (0.5, 1.0) \\ 240 & z \in [0.1, 0.5], \end{cases} \quad (46)$$

and the background concentration profile is given by

$$c_0(z) = \begin{cases} 4z & z \in (0, 0.5] \\ 2.5 - 8(z - 0.75)^2 & z \in (0.5, 1.0). \end{cases} \quad (47)$$

Table 3. Characteristics of the inclusion reconstructed by the conjugate gradient algorithm when the inclusion is placed in a region with vanishing temperature gradient. The real values for those variables are $z_0 = 0.25$, $\delta z = 0.08$, $\delta c = 1.20$ and $\delta z \delta c = 0.096$. The numbers in parentheses denote the relative error in percentage between the reconstructed parameters and their true values.

Noise	z_0 (error in %)	δz (error in %)	δc (error in %)	$\delta z \delta c$ (error in %)
0.00%	0.280 (12.0)	0.080 (0.0)	1.202 (0.2)	0.0962 (0.2)
0.05%	0.280 (12.0)	0.081 (1.3)	1.180 (1.7)	0.0956 (0.4)
0.10%	0.280 (12.0)	0.083 (3.8)	1.144 (4.7)	0.0950 (1.1)
1.00%	0.280 (12.0)	0.091 (14.0)	1.026 (15.0)	0.0933 (2.8)

Table 4. Characteristics of the inclusions in the two-particle model reconstructed from noise free data. The initial guess is $z_1 = 0.32$, $\delta z_1 = 0.05$, $\delta c_1 = 0.8$ and $z_2 = 0.28$, $\delta z_2 = 0.10$, $\delta c_1 = 1.0$. The numbers in parentheses denote the relative error in percentage between the reconstructed parameters and their true values.

Gas	z_i (error in %)	δz_i (error in %)	δc_i (error in %)	$\delta z_i \delta c_i$ (error in %)
$i = 1$	0.200 (0.0)	0.060 (0.0)	1.002 (0.2)	0.0601 (0.2)
$i = 2$	0.250 (0.0)	0.081 (1.3)	1.190 (0.8)	0.0964 (0.4)

Table 5. Same as table 4 with 0.10% noise.

Gas	z_i (error in %)	δz_i (error in %)	δc_i (error in %)	$\delta z_i \delta c_i$ (error in %)
$i = 1$	0.200 (0.0)	0.059 (1.7)	1.012 (1.2)	0.060 (0.5)
$i = 2$	0.251 (0.4)	0.082 (2.5)	1.150 (4.2)	0.094 (1.8)

A small inclusion is placed at $z_0 = 0.25$. The width of the inclusion is $\delta z = 0.08$ and the concentration variation $\delta c = 1.2$.

Reconstructions from data at different noise levels by the conjugate gradient method are presented in table 3. The gradients have been computed by using a finite difference approximation. We found numerically that while we can recover δc and δz almost perfectly with exact simulated data, the exact location z_0 is not retrieved if our initial guess lies within \mathcal{I} . The initial guess for the data in table 3 was chosen to be $z_0 = 0.28$, $\delta z = 0.07$, and $\delta c = 1.0$.

5.2. The case of two gases

Let us now consider the case of two gases. We use (42) and (47) as the background profiles for the two gases, respectively. The characteristics for the two small inclusions are the following: $(z_1, \delta z_1, \delta c_1) = (0.30, 0.06, 1.00)$ and $(z_2, \delta z_2, \delta c_2) = (0.25, 0.08, 1.20)$. We simulate the data using 800 wavenumbers uniformly distributed in two band centred at $\nu_1 = 1500 \text{ cm}^{-1}$ and $\nu_2 = 2000 \text{ cm}^{-1}$, respectively. The absorption kernel has the form given in (13) with parameters given by $\bar{\alpha} = 2 \times 10^{-2}$, and $(Q_{11}, Q_{12}, Q_{21}, Q_{22}) = (2.0, 1.0, 1.0, 2.0) \times 10^{-2}$.

We perform three sets of numerical experiments with noise free data, data with 0.1% noise and data with 1% noise, respectively. The results are listed in tables 4, 5 and 6, respectively. The initial guess is $z_1 = 0.32$, $\delta z_1 = 0.05$, $\delta c_1 = 0.8$ and $z_2 = 0.28$, $\delta z_2 = 0.10$, $\delta c_1 = 1.0$. We found that the initial guess on the positions may be chosen relatively far away from the true values, while the guess on the other two parameters should be close to the true value in order for the CG algorithm to converge.

Note in table 4 that the parameters for both inclusions are recovered very accurately in the absence of noise. This is quite similar to the one-particle case. The only noticeable

Table 6. Same as table 4 with 1% noise.

Gas	z_i (error in %)	δz_i (error in %)	δc_i (error in %)	$\delta z_i \delta c_i$ (error in %)
$i = 1$	0.204 (2.0)	0.053 (12.0)	1.081 (8.1)	0.057 (4.5)
$i = 2$	0.261 (4.4)	0.089 (11.0)	1.038 (14.0)	0.092 (3.8)

difference numerically is that a much wider range of wavenumbers is necessary in the case of multiple particles to ensure convergence. This is in agreement with theory, which indicates that the number of measurements should scale at least linearly with the number of retrieved gas profiles.

At moderate levels of noise, we can still recover the positions of the inclusions and their strength $\delta c \delta z$, but not δc and δz separately. We also observed in our simulations that, as the noise level increases, we even lose the information about z_0 and $\delta z \delta c$. The only quantity which seems numerically to be accurately reconstructed is then p introduced in (41).

6. Conclusions and remarks

Under some separation assumptions on the spectral emission coefficient, we have shown that the concentration profiles of single or multiple gases could uniquely be reconstructed from radiation measurements. Moreover we have shown that the reconstruction invokes the inversion of a Laplace transform (at best) and is therefore a severely ill-posed problem. The assumptions on the emission coefficient necessary to obtain an explicit formula are technical and should not modify the general conclusion that the reconstruction problem is *severely ill-posed* even in more general settings.

To reconstruct localized strong fluctuations such as ozone layers in the troposphere, we have presented an asymptotic model, which assesses the type of information that can be reconstructed based on the quality of the measured data. For instance, we show that with moderate noise levels, we can reconstruct the location of the inclusion and the product of its thickness with its concentration variation (with respect to the background). We have shown that the reconstruction of both the thickness and the concentration variation requires much more accurate data.

We have conducted numerical experiments on academic though qualitatively faithful benchmarks that corroborate the theory. Our main conclusion is that the reconstruction of the thickness and the concentration of ozone layers in the troposphere requires extremely accurate data. In our setting, possible errors in the reconstruction of the background are treated as noise in the measured data. This assumption certainly needs improvement. Yet the method of asymptotic expansions presented in this paper provides a systematic framework to evaluate the type of information that can be retrieved on localized inclusions from measured data with a given noise level.

Acknowledgments

We would like to thank Kevin Bowman from Jet Propulsion Laboratory (JPL) for introducing us to the retrieval problem during an industrial workshop organized at IPAM and for numerous stimulating discussions on the subject. We also acknowledge useful recommendations made by anonymous referees. This work was conducted while the authors were visiting the Institute for Pure and Applied Mathematics (IPAM) at UCLA. We would like to thank IPAM for their hospitality and generous support. This work was funded in part by NSF grant DMS-0239097. GB acknowledges support from an Alfred P Sloan fellowship.

References

- [1] Ammari H and Kang H 2004 *Reconstruction of Small Inhomogeneities from Boundary Measurements (Lecture Notes in Mathematics)* (Berlin: Springer)
- [2] Bal G 2003 Optical tomography for small volume absorbing inclusions *Inverse Problems* **19** 371–86
- [3] Beer R, Glavich T and Rider D 2001 Tropospheric emission spectrometer for the Earth observing system's Aura satellite *Appl. Opt.* **40** 2356–67
- [4] Bertero M and Pike E R 1993 Signal processing for linear instrumental systems with noise: a general theory with illustrations from optical imaging and light scattering problems *Handbook of Statistics* ed V N K Bose and C R Rao (Amsterdam: Elsevier) pp 1–46
- [5] Bowman K, Worden J, Steck T and Worden H M 2002 Capturing time and vertical variability of tropospheric ozone: a study using TES nadir retrievals *J. Geophys. Res.* **107** 4723–34
- [6] Cedio-Fengya D J, Moskow S and Vogelius M S 1998 Identification of conductivity imperfections of small diameter by boundary measurements, continuous dependence and computational reconstruction *Inverse Problems* **14** 553–94
- [7] Clerbaux C, Hadji-Lazaro J, Payan S, Camy-Peyret C, Wang J, Edwards D P and Luo M 2002 Retrieval of CO from nadir remote-sensing measurements in the infrared by use of four different inversion algorithms *Appl. Opt.* **41** 7068–78
- [8] Conway J B 1978 *Functions in One Complex Variable I (Graduate Texts in Mathematics)* (New York: Springer)
- [9] Doicu A, Schreier F and Hess M 2004 Iterative regularization methods for atmospheric remote sensing *J. Quantum Spectrosc. Radiat. Transfer.* **83** 47–61
- [10] Engl H W, Hanke M and Neubauer A 1996 *Regularization of Inverse Problems* (Dordrecht: Kluwer)
- [11] Friedrichs K O 1985 *Advanced Ordinary Differential Equations* (New York: Taylor and Francis)
- [12] Goody R M and Yung Y L 1989 *Atmospheric Radiation: Theoretical Basis* 2nd edn (New York: Oxford University Press)
- [13] Huang X, Yung Y L and Margolis J S 2003 Use of high-resolution measurements for the retrieval of temperature and gas-concentration profiles from outgoing infrared spectra in the presence of cirrus clouds *Appl. Opt.* **42** 2155–65
- [14] Kryzhniy V V 2003 Direct regularization of the inversion of real-valued Laplace transforms *Inverse Problems* **19** 573–83
- [15] Liou K 2002 *An Introduction to Atmospheric Radiation* 2nd edn (Boston: Academic)
- [16] McCartney E J 1983 *Absorption and Emission by Atmospheric Gases: The Physical Processes* (New York: Wiley)
- [17] Miller K 1970 Least-squares method for ill-posed problems with a prescribed bound *SIAM J. Math. Anal.* **1** 52–74
- [18] Rodgers C 2000 *Inverse Methods for Atmospheric Sounding: Theory and Practice* (Singapore: World Scientific)
- [19] Rudin W 1974 *Real and Complex Analysis* 2nd edn (New York: McGraw-Hill)
- [20] Steck T 2002 Methods for determining regularization for atmospheric retrieval problems *Appl. Opt.* **41** 1788–97
- [21] Trefthen L N and Bau D 1997 *Numerical Linear Algebra* (Philadelphia, PA: SIAM)
- [22] Vogel C R 2002 *Computational Methods for Inverse Problems (Frontiers in Applied Mathematics)* (Philadelphia, PA: SIAM)
- [23] Vretblad A 2003 *Fourier Analysis and Its Applications (Graduate Texts in Mathematics)* (New York: Springer)